Journal of Electroanalytical Chemistry 904 (2022) 115941

Contents lists available at ScienceDirect

Journal of Electroanalytical Chemistry

journal homepage: www.elsevier.com/locate/jelechem

A tattoo-like glucose abiotic biofuel cell

Saikat Banerjee, Gymama Slaughter *

Center for Bioelectronics, Department of Electrical and Computer Engineering, Old Dominion University, Norfolk, VA 23528, USA

ARTICLE INFO

Keywords:
Biofuel cell
Abiotic
Glucose
Platinum
Silver oxide nanoparticles
Carbon nanotubes

ABSTRACT

Glucose abiotic biofuel cell using gold nanoparticles (AuNPs) ink printed electrodes on bacterial nanocellulose was developed with colloidal platinum (co-Pt) anode and silver oxide/multiwalled carbon nanotube (Ag_2O-MWCNTs) nanocomposite cathode. The co-Pt was electrodeposited to increase the conductivity of the printed AuNPs electrode and enhance the oxidation of glucose at the anode. The Ag_2O-MWCNT composite was synthesized and modified on the cathode surface to provide a porous conductive network and increase the electrode electrocatalytic activity. The surface morphologies and electrochemical properties were characterized using scanning electron microscopy (SEM), cyclic voltammetry (CV), and linear sweep voltammetry (LSV). An open circuit voltage (V_{oc}) of 0.43 V, short circuit current density (I_{sc}) of 0.405 mA/cm^2, and maximum power density (P_{max}) of 0.055 mW/cm^2 at 0.23 V were achieved in the presence of 5 mM glucose, whereas a higher V_{oc} of 0.57 V, I_{sc} of 0.581 mA/cm^2, and P_{max} of 0.087 mW/cm^2 at 0.35 V were obtained in the presence of 20 mM glucose. Using various glucose concentrations, the peak power density increased linearly and showed good performance in serum containing glucose. This single abiotic biofuel cell generated adequate power via a voltage booster circuit to illuminate an LED.

1. Introduction

Glucose biofuel cells convert the chemical energy stored in glucose fuel into electrical energy through an electrochemical reaction and is considered as one of the most promising technologies for generating bioelectricity [1–7]. They are environmentally friendly, biocompatible, small in form factor, and their use as analytical devices has increased because of their capability to serve as diagnostic tools [8–10]. A key advantage of glucose biofuel cells is that at ambient temperature and neutral pH conditions, they demonstrate high conversion efficiency and have been demonstrated to generate adequate bioelectricity to power small electronic devices [11]. The two types of commonly developed biofuel cells are the enzymatic biofuel cell and the non-enzymatic biofuel cell. Enzymatic biofuel cell uses complex enzyme immobilization strategies to immobilize enzymes to the surface of electrode material. The enzyme stability is widely affected by pH and temperature, which can result in enzyme denaturation if the microenvironment conditions are not optimal. To address the current limitations associated with enzymatic glucose biosensors, conductive materials such as carbon nanotubes [12,13], metal oxides [14,15], nanostructured materials [16,17], and graphene [18] are being explored as an alternative sensing material for glucose and molecular oxygen oxidation and reduction, respectively. Noble metals such as gold, platinum and silver nanoparticles have gained significant attention because of their unique electrocatalytic properties [19,20]. These nanoparticles have been shown to improve the direct electron transfer, signal transduction, and efficiency of sensors when used as the sensing material. Platinum nanoparticles (PtNPs) and nanocomposites have been shown to have the capacity to directly electrooxidize glucose even in the absence of enzymes and mediators [21,22]. The large surface area offered by nanoparticles, specifically colloidal platinum in biofuel cells makes them attractive for the construction of glucose sensors [21,22].

There is a growing demand for flexible electronics that integrate miniaturized components to realize analytical devices on conformal substrates. The application of bacterial nanocellulose (BNC) thin film has garnered attention in biomedical, flexible electronics, separation, and waste purification research due to its high mechanical strength and flexibility [23]. BNC exhibits transferable tattoo-like properties, such as good shape retention, high water-binding capacity, and higher surface area when compared to native cellulose [24,25]. These unique properties facilitate the use of BNC in the fabrication of several different products like membrane, high-grade paper, speaker diaphragm, diet food, and textiles. Current research on BNC focuses on the incor-

* Corresponding author at: Bioelectronics Laboratory, Center for Bioelectronics, Old Dominion University, Department of Electrical and Computer Engineering, 4211 Monarch Way, Norfolk, VA 23508, USA.
E-mail address: gslaught@odu.edu (G. Slaughter).

https://doi.org/10.1016/j.jelechem.2021.115941
Received 29 June 2021; Received in revised form 25 September 2021; Accepted 1 December 2021
Available online 6 December 2021

poration of inorganic and/ or organic nanomaterials to provide antibacterial, optical, electrical, magnetic, and catalytic properties for use in biomedical research [26]. The use of BNC as substrate or sensing material in the development of transferable tattoo-like biosensors and bioelectronics could be achieved using screen printing and inkjet printing strategies. These strategies offer several advantages over cleanroom microfabrication strategies, such as low processing costs, rapid processing rates, minimal waste generation, and low contamination [24,25].

Inkjet printing enables consistent large-scale production of arrays of conductive materials. The range of nanoparticles to biomolecules materials that can be printed with inkjet printers offer a means to mass produce functional components for biofuel cell. Inkjet printing of conductive and non-conductive materials enables the development of ultra-thin and compact analytical devices that may continue to revolutionize wearable and implantable devices in terms of cost, efficiency, and reproducibility.

In this work, we demonstrate an ultra-thin tattoo-like glucose abiotic biofuel cell system capable of generating adequate bioelectricity using a facile three-step fabrication process. The abiotic glucose biofuel cell was constructed by first printing gold nanoparticles (AuNPs) electrodes on 130 μm thin sheet BNC to serve as the anodic and cathodic base material, upon which we electrodeposited colloidal-Pt at the anode and drop casted a mixture of multiwalled carbon nanotubes (MWCNTs) and silver oxide nanoparticles (Ag_2O) on the cathode. The morphology of the electrode materials was characterized using scanning electron microscopy (SEM) and the electrochemical characterization was achieved via linear sweep voltammetry (LSV) and cyclic voltammetry (CV). This combination of anodic and cathodic sensing materials enables the direct oxidation of glucose at the anode and reduction of Ag_2O at the cathode to generate bioelectricity. The power generated by the tattoo-like glucose abiotic biofuel cell was linear over a concentration of 1 mM −10 mM. The electrical power generated from the single abiotic fuel cell was supplied to a voltage boost converter to amplify the voltage and illuminate a light emitting diode (LED). This facile approach demonstrates a low-cost alternative to mass producing analytical devices for biosensor and bioelectronics applications.

2. Experimental

2.1. Materials

Silver nitrate, polyethylene glycol 3000 (PEG), sodium hydroxide, D (+) glucose, potassium phosphate monobasic, sodium azide, and Nafion were obtained from Sigma-Aldrich. The platinizing solution was purchased from YSI Inc., and NGP-J gold nanoparticle ink was acquired from Iwatani Corporation of America. The multiwalled carbon nanotube NINK-1000 was obtained from Nanolab, Inc. Gluconacetobacter xylinus (ATCC 10245) was purchased from ATCC. Hydrosulphite of sodium medium (HS medium) was purchased from Himedia Laboratories. All the solutions were prepared with 18.2 MΩ-cm Milli-Q water. Platinum counter electrode, Ag/AgCl reference electrode, and PalmSense4 potentiostat were purchased from BASI Inc. The S882Z charge pump integrated circuit (IC) was obtained from Seiko Electronics.

2.2. Bacterial nanocellulose synthesis

Gluconacetobacter Xylinus culture was maintained in sterile HS medium as static cultures at 30 °C. Briefly, the cell pellet was rehydrated in HS medium and transfer to 50 mL conical tube containing 5 mL broth at 30 °C to establish a good growth for 72 h. To generate the inoculum, the pellicle was removed to disperse the cells by vortexing at maximum speed for 1 min. The suspended bacteria (1 mL each) solution was transferred to a fresh 50 mL HS medium in sterile 100 mm crystallization dishes. The inoculated crystallization dishes were incubated at 30 °C undisturbed for 1 week. The bacteria were fed at 1-week intervals by carefully adding 50 mL of HS medium to enable the formation of subsequent pellicles for a total of 6 weeks to form 6 uniform pellicles. To harvest the bacteria nanocellulose, the pellicles were incubated at 90 °C in 0.5 M NaOH for 1 h to denature the bacteria. The pellicles were extensively washed in Milli-Q water for 48 h to remove the NaOH and achieve neutral pH. The washed pellicles were stored 0.02% sodium azide solution at 4 °C prior to use.

2.3. Electrode fabrication

The bacterial nanocellulose pellicles were placed on 3-inch PET wafers, smoothened in Milli-Q water to remove all air bubbles, and allowed to dry at room temperature overnight prior to printing on the BNC substrate. Fig. 1A provides the illustration of the electrode pattern with an overall dimension of 15 mm × 10 mm designed using CoralDRAW. A semicircle and a larger circle (r = 5 mm) shape design were implemented for the cathode and anode, respectively. The .bmp file was exported to the Fujifilm Dimatix 2850 Materials Printer to be converted to a.tf file for printing. The software then was configured with the thickness of the substrate (130 μm bacterial nanocellulose on PET), printing layers (2 layers), and jetting speed (50 Hz) for printing the electrodes. The NGP-J gold ink (650 μL) was injected into a DMC-11610 cartridge (10 pL drop-size) tank using a syringe followed by capping of the cartridge with the nozzle head. The platen and cartridge temperatures were set at 45 °C and 28 °C. A printing resolution of 1016 DPI was used, with the jetting voltage range between 22 and 25 V and all 16 jets were used. After printing, the substrate was dried in a conventional oven for 90 min at 85 °C to dry the ink, and then cooled to cool temperature overnight before the preparation of the biofuel cell.

2.4. Synthesis of silver oxide nanoparticles

Silver oxide nanoparticles (Ag_2O) solution was prepared by dissolving 20 g of PEG in 1 L of Milli-Q water, which was then heated to 75 °C under constant stirring for 1 h to ensure that all the PEG was completely dissolved to form a homogeneous solution. The resulting PEG solution was filtered using Whatman ashless filter papers to remove any impurities. Under constant stirring, silver nitrate solution was prepared from 0.5 g of silver nitrate and was added to the prepared PEG

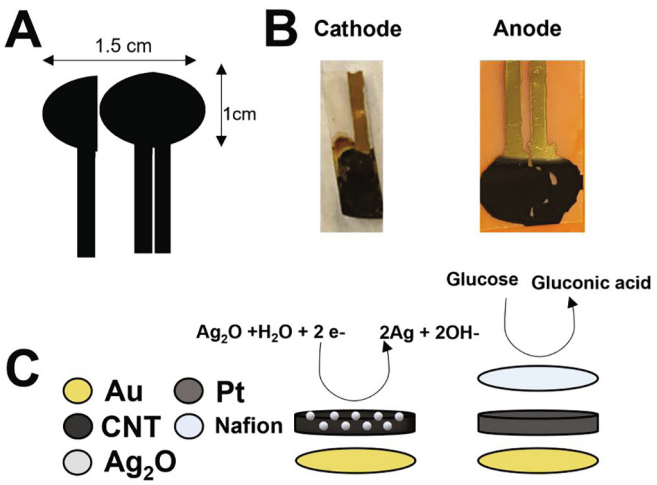

Fig. 1. (A) Design pattern of electrodes. (B) Fabricated Au-*co*-Pt anode and Ag2O-MWCNTs cathode. (C) Schematic illustration of the anodic and cathodic reaction mechanisms.

solution at 75 °C for 1 h. The pH was maintained at pH 9.8 to 10 throughout the reaction process using 0.1 M NaOH solution. Subsequently, the Ag_2O particles precipitated to the bottom of the solution and the solution was centrifuged to extract the particles from the original solution. A 20 μL of MWCNTs solution was mixed in with the Ag_2O particles using ultra-sonication for 30 min to form the Ag_2O-MWCNTs solution.

2.5. Preparation of glucose abiotic biofuel cell

The dried printed electrodes were rinsed with isopropanol (IPA) for 5 min and dried with nitrogen gas to remove any impurities from the surface. Colloidal platinum (co-Pt) was electrodeposited on the anodic electrode using a three-electrode configuration consisting of the anodic working electrode, platinum counter electrode, and Ag/AgCl reference electrode immersed in platinizing solution. The co-Pt was electrodeposited onto the surface on the printed gold electrode at an applied potential of − 225 mV vs. Ag/AgCl for 1500 s. The electrode was then washed with Milli-Q water and dried a 80 °C for 30 min, followed by cooling in ambient air as shown in Fig. 1B. The Ag_2O-MWCNTs solution was drop-casted onto the cathode surface, followed by soft baking at 60 °C for 30 min. Fig. 1C provides a schematic illustration of the process involved in preparation of the anodic and cathodic functional components of the glucose abiotic biofuel cell. For easy handling and device testing, a tungsten wire was attached to the electrodes using carbon wire glue.

2.6. Characterization of printed electrodes

Scanning electron microscopy (SEM) images were taken using a Hitachi FE-SEM Su-70. The cyclic voltammograms (CV) and linear sweep voltammograms of the fabricated abiotic biofuel cell responses to phosphate buffer solution (PBS) and glucose or oxygen were observed using a PalmSense4 electrochemical system. The inkjet-printed electrode on BNCs served as working electrodes. A platinum wire and Ag/AgCl served as the counter electrode and reference electrode, respectively. All measurements were carried out in 0.1 M PBS solution, pH 7.4 using an electrochemical cell.

3. Results and discussion

Inkjet printing was performed to pattern gold nanostructures on the BNC thin film. The gold surface on the BNC was characterized by scanning electron microscopy (SEM). Fig. 2A shows the printed gold electrode surface. The gold electrode surface exhibited a plain surface with nanostructures (ϕ = 22.4 ± 6.2 nm), thereby making it ideal for use as electrode substrate material. From Fig. 2B, the electrodeposition was performed to deposit co-Pt on the printed gold electrode. The electrodeposited co-Pt presented a fractal-like distribution of microstructures, measuring on average 3.8 ± 1.1 μm in diameter. The co-Pt structures were found to be uniformly deposited on the printed gold surface. They also exhibited a porous morphology with a high surface area to volume ratio and appear to be composed of nanostructures. The co-Pt structures act as an inorganic catalyst at the electrode–electrolyte interface to improve the catalysis of glucose at the anode when compared to the bare printed gold electrode. Fig. 2C shows the Ag_2O-MWCNTs nanocomposite drop casted on the printed gold electrode. A network of MWCNTs (ϕ = 53 ± 0.8 nm) intertwined with the Ag_2O nanostructures with diameters ranging from 12 nm to 389 nm was observed. Smaller Ag_2O nanostructures were observed to be directly attached to the MWCNTs surface. This interconnected network of Ag_2O-MWCNTs nanocomposite is essential in creating a porous environment to enable Ag_2O reduction at the cathode [6].

3.1. Electrochemical characterization

The cyclic voltammogram in Fig. 3 shows the electrooxidation of glucose in the presence of co-Pt electrodeposited on printed gold nanostructures to produce gluconic acid and electrons according to Eq. (1) [27].

$$\text{Glucose} + \text{Au} - \text{co} - \text{Pt} \rightarrow \text{Gluconic Acid} + 2H^+ + 2e^- \quad (1)$$

At the anodic electrode, hydrogen adsorbed to the co-Pt electrode surface and the co-Pt acts as the dehydrogenation site wherein the gold nanostructure surface facilitates the regeneration of co-Pt from poisoning due to adsorbed intermediates from the oxidation of glucose. At the onset potential of −0.428 V, surface Pt-OH particles are formed which oxidizes the intermediates produced by the absorption of glucose, and thus frees up active Pt sites for direct oxidation of glucose [28]. During the electrooxidation of the glucose, a well-defined peak was observed around a potential of −0.052 V with higher current density of 1.435 mA/cm^2 in comparison to the current density of 0.85 mA/cm^2 in the absence of glucose. The presence of an oxidation peak is attributed to the electron transfer occurring at the gold co-Pt surface in the presence of glucose. This shows that co-Pt exhibits a catalytic effect in the direct oxidation of glucose. Therefore, the electrodeposition of co-Pt on the gold printed BNC provides large surface area decorated with nanostructures to enhance the electrocatalytic performance of the anode. The offset panel in Fig. 3 shows the linearity of the peaks from 2 mM to 28 mM glucose (r^2 = 0.9883) with a sensitivity of 35.01 μA/mM-cm^2 and a limit of detection of 0.88 mM (3 S/N).

In general, oxygen reducing enzymes such as bilirubin oxidase and laccase are used at the cathode to catalyze the reduction of oxygen to produce water and transfer the electrons generated to the current collector [7,8]. The possibility of the enzyme becoming denatured under environmental conditions and the low solubility of dissolved oxygen in solution causes the enzyme-based cathodes to exhibit a low performance in air and, and thus require measurements to be taken under stirring conditions [29]. The Ag_2O-MWCNT composite is used here as an alternative cathode material and thus serves as the cathodic electron acceptor in the biofuel cell. Ag_2O accepts the electrons generated at the anode and is reduced to Ag. As Ag_2O is reduced to Ag, hydroxyl (OH–) is generated as depicted in Equation 2.

$$Ag_2O + H_2O + 2e^- \rightarrow 2Ag + 2OH^- \quad (2)$$

Fig. 4 shows the electrocatalytic behavior of the Ag_2O-MWCNT cathode in a non-stirring air-saturated PBS. The shape of the voltammogram is consistent with those previously reported [30]. The electrode was then placed under oxygen purging for 5 and 10 min to achieve oxygen saturation conditions. From the voltammogram, the reduction current density of Ag_2O-MWCNT cathode increases in the presence of oxygen with an onset potential of 0.231 V in a similar manner to oxygen reduction at noble metal or enzyme-based cathodes [4]. The reduction peak observed is due to the presence of silver, which results from the reduction reaction of Ag_2O in the Ag_2O-MWCNT electrode and is independent of the electrolyte environment and can be described by the reaction mechanism in Eq. (2). In addition, the Ag_2O can then be slowly regenerated through exposure to air/oxygen at room temperature, thereby slowly restoring Ag_2O to be reduced again in PBS electrolyte [31]. The electrocatalytic behavior observed can also be attributed to the improved porosity provided by the integration of MWCNTs with Ag_2O to enable the reduction and facilitate electron transfer [32]. This anodic and cathodic reactions also indicate successful direct electron transfer for the co-Pt and Ag_2O-MWCNTs electrodes. The co-Pt glucose oxidation anode and the Ag_2O-MWCNTs Ag_2O reduction cathode were assembled as a two-electrode system to evaluate the biofuel cell performance. The oxidation reaction at the

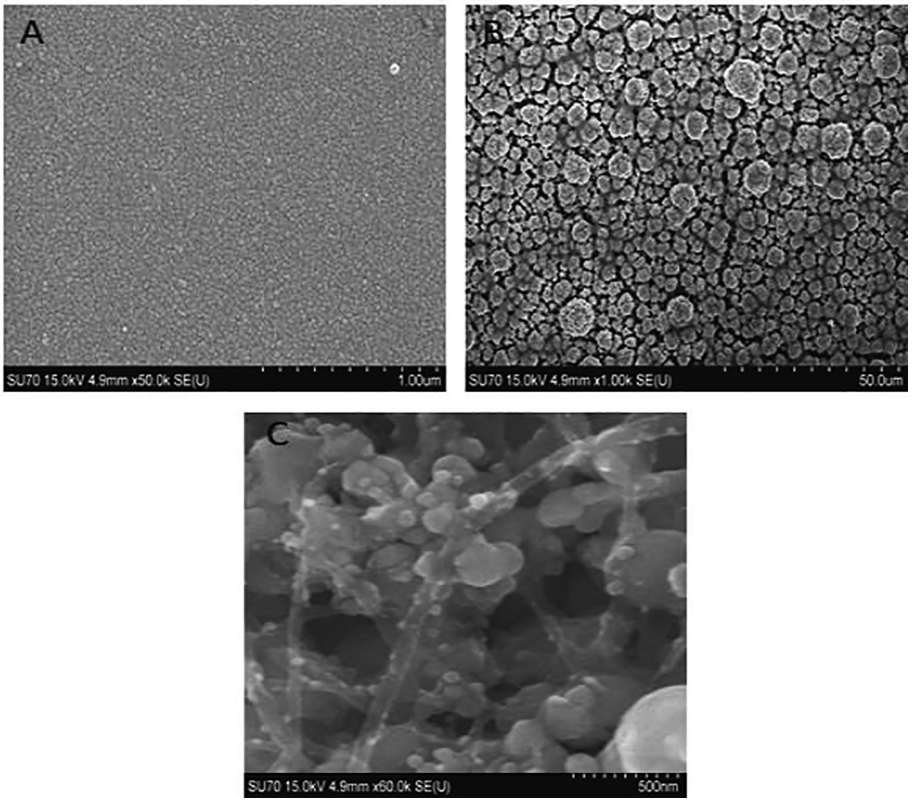

Fig. 2. Scanning electron micrographs of (A) bare printed gold nanoparticles (AuNPs) on bacterial nanocellulose sheet, (B) colloidal platinum (co-Pt) electrodeposited on printed gold nanostructures, (C) sliver oxide-multiwalled carbon nanotubes (Ag_2O -MWCNTs) nanocomposite drop cast on printed Au electrode.

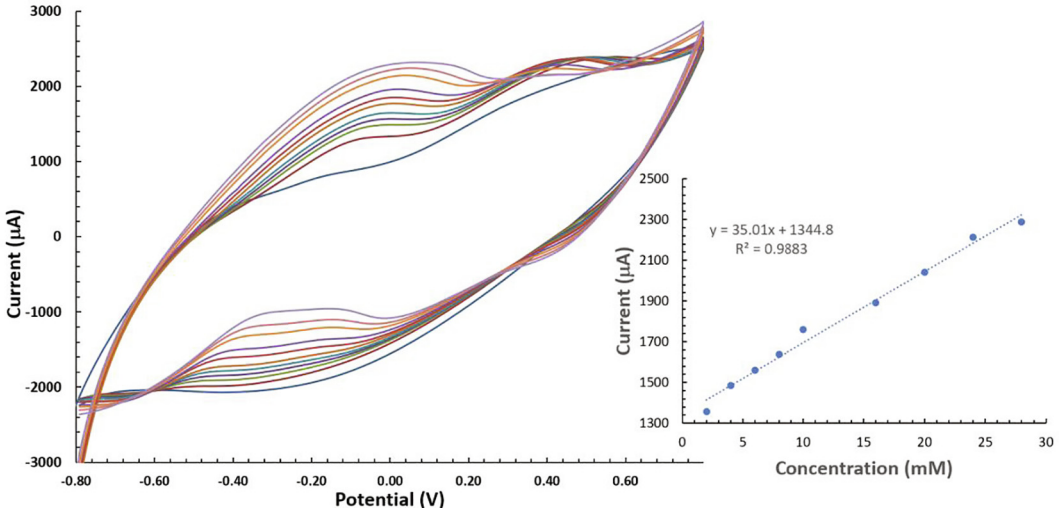

Fig. 3. Cyclic voltammogram of gold co-Pt anode in the absence and presence of 2–20 mM glucose. The offset panel shows the linearity of the anodic peaks for the co-Pt anode. 0.1 M PBS pH 7.4 and 50 mV/s against Ag /AgCl.

anode produces electrons that travels through the external circuitry and the ions move through the electrolyte and recombines at the cathode for the reduction of Ag_2O to generate a stable current.

3.2. Biofuel characterization

The abiotic biofuel cell was constructed with the co-Pt anode and Ag_2O-MWCNT composite cathode arrange side by side on a PET substrate to provide structural support for characterization. The biofuel cell was placed in a beaker containing various concentrations of glucose. The open circuit potential of the anode and cathode measured against Ag/AgCl were −0.436 V and 0.218 V, respectively. The anode potential was lower than the cathode potential and were similar to the onset potentials in the CVs of Figs. 3 and 4. The membraneless biofuel cell was assembled as shown in Fig. 5A insert. Glucose electrolyte solutions ranging from 1 mM to 20 mM were prepare with in PBS. The polarization performance of the biofuel cell is shown in Fig. 5A. The co-Pt anode was used as the negative electrode and the Ag_2O-MWCNTs

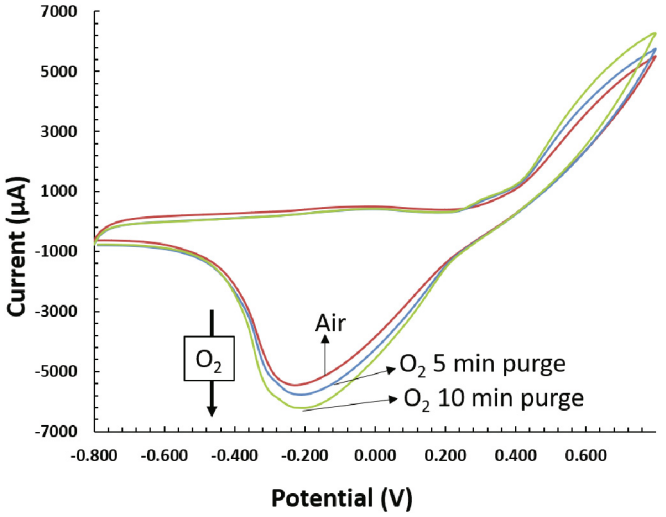

Fig. 4. Cyclic voltammogram of CNT-Ag_2O cathode in PBS with O_2 saturated PBS for 5 min and 10 min. 0.1 M PBS pH 7.4 and 50 mV/s against Ag /AgCl.

cathode was used as the positive electrode. The polarization curves were measured using linear sweep voltammetry (LSV) and power density curves were acquired to determine the peak power of the abiotic biofuel cell. The open-circuit voltage (V_{oc}) of the biofuel cell was 0.43 V and the short current density was 0.405 mA/cm^2 when operating on 5 mM glucose, although the V_{oc} was smaller than the expected maximum theoretical thermodynamic redox potential for glucose oxidation and Ag_2O reduction [33]. However, the high current observed is attributed to the increased surface area caused by the incorporation of nanostructures on the printed gold substrate.

Fig. 5B presents the power density profiles. The peak power densities achieved in 5 mM and 20 mM glucose were 0.055 mW/cm^2 at a cell voltage of 0.23 V and 0.087 mW/cm^2 at 0.35 V, respectively. The obtained power densities were the result of the decoration of the highly conductive printed AuNPs with electrodeposited co-Pt or Ag_2O-MWCNTs on the surface of the electrodes, which further improve the overall conductivity of the electrodes and provide a porous structure to enable the catalysis of glucose and Ag_2O. The glucose biofuel cell output power response was collected in triplicates and the calibration curve is shown in Fig. 6A. The biofuel cell exhibited a curve that has a linear response over a range of glucose concentrations from 1 mM to 10 mM (r^2 = 0.9458) with a detection sensitivity of 7.84 μW/mM-cm^2. Although the linear response to increasing glucose concentration is narrow, this result illustrates that the biofuel cell can be used as a glucose indicator [34,35]. Most glucose biosensors and other electrochemical devices require interfacing to bulky electrochemical workstations, which make them not well-suited for wearable applications. This alternative glucose indicator reduces the number of circuit components and complexity of the measuring circuit, thereby the overall cost. An attractive advantage of this type of glucose indicator is that it can serve as a power source to a low-powered wireless communication electronics while at the same time sensing glucose.

Furthermore, the glucose abiotic biofuel cell was setup using serum solution as an electrolyte and the polarization curve and power output were recorded (Fig. 6B). The glucose concentrations of serum were 1 mM and 5 mM. The peak power output was observed to be 0.045 mW/cm^2 at 0.21 V in serum as shown in Fig. 6B. This value was obviously smaller as compared with the oxidation of 5 mM glucose solution. The fall in power from the 0.055 mW/cm^2 at 0.23 V observed for 5 mM glucose could be due to the interaction of protein molecules present in the serum electrolyte solution with the electrode surfaces, thereby inhibiting the catalytic reaction [36]. The porosity of the nanocellulose enables the vertical wicking of glucose fluid from the source to the active area of the electrodes to enable the redox reaction to take place in the presence of glucose. As it is seen in Fig. 6C, the fabricated abiotic biofuel cell was moistened with Milli-Q water and placed on the skin with the electroactive side in direct contact with the skin to form a tattoo-like substrate on the skin. As soon as the water dried up, the sensor conformed to the skin (lower arm). In addition, the biofuel cell assembly was connected to a charge pump integrated circuit (S-882Z) through resistor, capacitor, and light emitting diode (LED). The voltage generated by the single biofuel cell was fed into the charge pump circuit, which then charges and discharges the charge pump through an output capacitor (0.1 μF) to increase the nominal input voltage to 1.8 V and illuminate the LED as shown in Fig. 6C. These results confirm that the fabricated co-Pt and Ag_2O-MWCNTs decorated printed gold electrodes are promising and desirable for abiotic glucose biofuel cell applications.

4. Conclusion

We fabricated an abiotic biofuel cell that consists of a glucose oxidizing co-Pt anode and Ag_2O reducing Ag_2O-MWCNTs cathode fabricated on the surface of gold inkjet-printed on a thin-film of nanocellulose synthesized via bacteria G. xlyinus. The electrodeposited co-Pt and the Ag_2O-MWCNTs composite were incorporated on the inkjet-printed gold nanoparticles electrodes to promote the catalysis, direct electron transfer, and improve conductivity in the electrodes. The results show that the fabricated electrodes could oxidize glucose and reduce Ag_2O, thereby producing good power density under physiological conditions as well as generating a stable voltage output to illuminate an LED circuit. The electrodeposition of co-Pt on printed gold improved the catalysis of glucose and the Ag_2O-

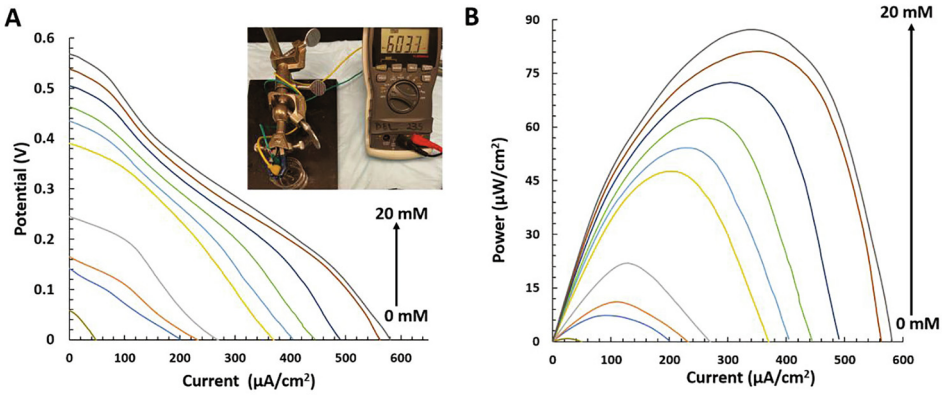

Fig. 5. (A) IV characteristic and (B) Power density curves of glucose biofuel cell operating on increasing concentration of glucose [0–20 mM] in 0.1 M PBS pH 7.4.

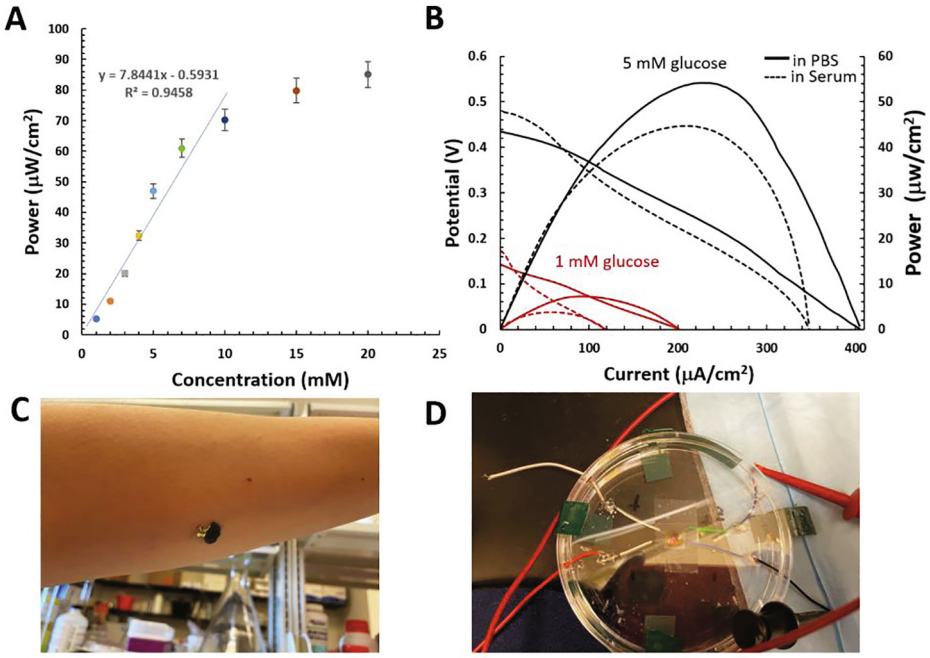

Fig. 6. (A) Calibration curve for abiotic biofuel cell with error bars (triplicates). (B) Polarization and power curves in serum and glucose solutions. (C) The abiotic biofuel cell electrodes perfectly conform to the skin without any adhesives. (D) A single biofuel cell serving as the power source to the charge pump integrated circuit (S882Z) connected to a load resistor and 0.1 μF capacitor and an LED.

MWCNTs composite drop-casted on the printed gold improved the performance of the abiotic biofuel cell. The biofuel cell exhibited high power output of 0.087 mW/cm^2 at 0.35 V in 20 mM glucose. The results also show a high output power performance in the 1 to 10 mM range with a sensitivity of 7.84 μW/mM-cm^2, which correlated to good glucose sensing performance and exhibit good power output profile. The maximum power output obtained were 0.055 mW/cm^2 in 5 Mm glucose and 0.045 mW/cm^2 in serum containing 5 mM glucose. The facile method presented for the fabrication of the electrodes has the potential to enable the realization of printed abiotic biofuel cell devices that provides a path to the mass production of cost-effective biofuel cells.

Declaration of Competing Interest

The authors declare that they have no known competing financial interests or personal relationships that could have appeared to influence the work reported in this paper.

Acknowledgment

The research presented in this article was supported by the National Science Foundation Award #1921364 and #1925806.

References

[1] K. Sharma, Carbohydrate-to-hydrogen production technologies: a mini-review, Renew. Sustain. Energy Rev. 105 (2019) 138–143.
[2] G. Pandey, Biomass based bio-electro fuel cells based on carbon electrodes: an alternative source of renewable energy, Sn Appl. Sci. 1 (5) (2019) 408.
[3] A. Nasar, R. Perveen, Applications of enzymatic biofuel cells in bioelectronic devices–A review, Int. J. Hydrogen Energy 44 (29) (2019) 15287–15312.
[4] L. Fu, J. Liu, Z. Hu, M. Zhou, Recent advances in the construction of biofuel cells based self-powered electrochemical biosensors: a review, Electroanalysis 30 (11) (2018) 2535–2550.
[5] G. Slaughter, T. Kulkarni, Enzymatic glucose biofuel cell and its application, J. Biochips Tissue Chips 5 (1) (2015) 1.
[6] A. Arsalis, A comprehensive review of fuel cell-based micro-combined-heat-and-power systems, Renew. Sustain. Energy Rev. 105 (2019) 391–414.
[7] A. Arshad, H.M. Ali, A. Habib, M.A. Bashir, M. Jabbal, Y. Yan, Energy and exergy analysis of fuel cells: a review, Therm. Sci. Eng. Progr. 9 (2019) 308–321.
[8] C. Abreu, Y. Nedellec, O. Ondel, F. Buret, S. Cosnier, A.L. Goff, M. Holzinger, Towards eco-friendly power sources: in series connected glucose biofuel cells power a disposable ovulation test, Sens. Actuat. B Chem. 277 (2018) 360–364.
[9] G. Slaughter, Current Advances in biosensor design and fabrication, Encyclopedia of Analytical Chemistry: Applications Theory and Instrumentation (2006) 1–25.
[10] M. Gamella, A. Koushanpour, E. Katz, Biofuel cells–activation of micro-and macro-electronic devices, Bioelectrochemistry 119 (2018) 33–42.
[11] Q. Xu, F. Zhang, L.i. Xu, P. Leung, C. Yang, H. Li, The applications and prospect of fuel cells in medical field: a review, Renew. Sustain. Energy Rev. 67 (2017) 574–580.
[12] D. Ivnitski, K. Artyushkova, P. Atanassov, Surface characterization and direct electrochemistry of redox copper centers of bilirubin oxidase from fungi myrothecium verrucaria, Bioelectrochemistry 74 (1) (2008) 101–110.
[13] B. Haghighi, B. Karimi, M. Tavahodi, H. Behzadneia, Electrochemical behavior of glucose oxidase immobilized on Pd-nanoparticles decorated ionic liquid derived fibrillated mesoporous carbon, Electroanalysis 26 (9) (2014) 2010–2016.
[14] G. Slaughter, J. Sunday, Fabrication of enzymatic glucose hydrogel biosensor based on hydrothermally grown ZnO nanoclusters, IEEE Sens. J. 14 (5) (2014) 1573–1576.
[15] C.X. Guo, C.M. Li, Direct electron transfer of glucose oxidase and biosensing of glucose on hollow sphere-nanostructured conducting polymer/metal oxide composite, PCCP 12 (38) (2010) 12153–12159.
[16] H.B. Wang, H.D. Zhang, Y. Chen, Y. Li, T. Gan, H_2O_2-mediated fluorescence quenching of double-stranded DNA templated copper nanoparticles for label-free and sensitive detection of glucose, RSC Adv., 2015.
[17] L. Wang, J. Zheng, Y. Li, S. Yang, C. Liu, Y. Xiao, J. Li, Z. Cao, R. Yang, AgNP-DNA@ GQDs hybrid: new approach for sensitive detection of H2O2 and glucose via simultaneous AgNP etching and DNA cleavage, Anal. Chem. 86 (24) (2014) 12348–12354.
[18] B.o. Liang, L.u. Fang, G. Yang, Y. Hu, X. Guo, X. Ye, Direct electron transfer glucose biosensor based on glucose oxidase self-assembled on electrochemically reduced carboxyl graphene, Biosens. Bioelectron. 43 (2013) 131–136.
[19] P. Yang, L. Wang, Q. Wu, Z. Chen, X. Lin, A method for determination of glucose by an amperometric bienzyme biosensor based on silver nanocubes modified Au electrode, Sens. Actuators, B 194 (2014) 71–78.
[20] Y. Zhu, X. Zhang, J. Sun, M. Li, Y. Lin, K. Kang, Y. Meng, Z. Feng, J. Wang, Y. Zhu, A non-enzymatic amperometric glucose sensor based on the use of graphene frameworks-promoted ultrafine platinum nanoparticles, Microchim. Acta 186 (8) (2019) 1–10.
[21] M.Q. Hasan, R. Kuis, J.S. Narayanan, G. Slaughter, Fabrication of highly effective hybrid biofuel cell based on integral colloidal platinum and bilirubin oxidase on gold support, Sci. Rep. 8 (1) (2018) 1–10.
[22] A. Baingane, G. Slaughter, Enzyme-free self-powered glucose sensing system, In Proc. IEEE SENSORS, Oct. (2018) 1–4.

[23] N. Shah, M. Ul-Islam, W.A. Khattak, J.K. Park, Overview of bacterial cellulose composites: a multipurpose advanced material, Carbohydr. Polym. 98 (2) (2013) 1585–1598.
[24] W. Hu, S. Chen, J. Yang, Z. Li, H. Wang, Functionalized bacterial cellulose derivatives and nanocomposites, Carbohydr. Polym. 101 (2014) 1043–1060.
[25] J.M. Wu, R.H. Liu, Thin stillage supplementation greatly enhances bacterial cellulose production by Gluconacetobacter xylinus, Carbohydr. Polym. 90 (1) (2012) 116–121.
[26] A. Ashjaran, M.E. Yazdanshenas, A. Rashidi, R. Khajavi, A. Rezaee, A. Ashjaran, Overview of bio nanofabric from bacterial cellulose, J. Text. Inst. 104 (2013) 121–131.
[27] A. Abbadi, H. van Bekkum, Effect of pH in the Pt-catalyzed oxidation of D-glucose to D-gluconic acid, J. Mol. Catal. A: Chem. 97 (2) (1995) 111–118.
[28] X. Yan, X. Ge, S. Cui, Pt-decorated nanoporous gold for glucose electrooxidation in neutral and alkaline solutions, Nanoscale Res. Lett. 6 (2011) 1–6.
[29] T. Ikeda, Bioelectrochemical studies based on enzyme-electrocatalysis, E Electrochimica acta 82 (2012) 158–164.
[30] Y. Wang, T. Hosono, Y. Hasebe, Hemin-adsorbed carbon felt for sensitive and rapid flow-amperometric detection of dissolved oxygen, Microchim. Acta 180 (13-14) (2013) 1295–1302.
[31] X. Xie, M. Ye, P.C. Hsu, N. Liu, Criddle, C.S., Cui, Y. Microbial battery for efficient energy recovery. Proc. Natl. Acad. Sci. 110 (2013) 15925-15930.
[32] A.J. Bandodkar, J.M. You, N.H. Kim, Y. Gu, R. Kumar, A.V. Mohan, J. Kurniawan, S. Imani, T. Nakagawa, B. Parish, M. Parthasarathy, Soft, stretchable, high power density electronic skin-based biofuel cells for scavenging energy from human sweat, Energy Environ. Sci. 10 (7) (2017) 1581–1589.
[33] T. Kulkarni, N. Mburu, G. Slaughter, Characterization of a self-powered glucose monitor, Sens. Transducers 203 (8) (2016) 1.
[34] K.P. Prasad, Y. Chen, P. Chen, Three-dimensional graphene-carbon nanotube hybrid for high-performance enzymatic biofuel cells, ACS Appl. Mater. Interfaces 6 (5) (2014) 3387–3393.
[35] G. Slaughter, Fabrication of nanoindented electrodes for glucose detection, J. Diabetes Sci. Technol. 4 (2) (2010) 320–327.
[36] C. Köhler, L. Bleck, M. Frei, R. Zengerle, S. Kerzenmacher, Poisoning of highly porous platinum electrodes by amino acids and tissue fluid constituents, ChemElectroChem 2 (11) (2015) 1785–1793.